POLITECNICO DI TORINO
Repository ISTITUZIONALE

Organic fouling in forward osmosis: Governing factors and a direct comparison with membrane filtration driven by hydraulic pressure

Original
Organic fouling in forward osmosis: Governing factors and a direct comparison with membrane filtration driven by hydraulic pressure / Ricceri, F., Giagnorio, M., Zodrow, K.R., Tiraferri, A.. - In: JOURNAL OF MEMBRANE SCIENCE. - ISSN 0376-7388. - 619:(2021), p. 118759. [10.1016/j.memsci.2020.118759]

Availability:
This version is available at: 11583/2852160 since: 2020-11-11T09:59:59Z

Publisher:
Elsevier B.V.

Published
DOI:10.1016/j.memsci.2020.118759

Terms of use:

This article is made available under terms and conditions as specified in the corresponding bibliographic description in the repository

Publisher copyright

(Article begins on next page)

10 October 2026

Organic fouling in forward osmosis: Governing factors and a direct comparison with membrane filtration driven by hydraulic pressure

Francesco Ricceri[1,2], Mattia Giagnorio[1], Katherine R. Zodrow[3], Alberto Tiraferri[1,2*]

1: Department of Environment, Land and Infrastructure Engineering, Politecnico di Torino, Corso Duca degli Abruzzi, 24 – 10129 Torino (Italy)

2: CleanWaterCenter@PoliTo, Corso Duca degli Abruzzi, 24 – 10129 Torino (Italy), web: http://cleanwater.polito.it/

3: Environmental Engineering Department, Montana Technological University, 1300 West Park Street, Butte, 59701 Montana (USA)

*Corresponding Author. Email: alberto.tiraferri@polito.it; Tel: +39-0110907628, Fax: +39-0110907611.

Abstract

The fouling behavior of osmotically-driven forward osmosis (FO) is widely believed to be superior with respect to hydraulic pressure-driven membrane applications, based on a number of experiments reported in the literature. However, experimental confounders often exist, preventing fair comparison between the different processes, one being the deployment of non-comparable membranes. This study systematically investigates the conditions influencing organic fouling in FO and compares the behavior in FO and in a hydraulic pressure-driven process, under equivalent conditions. The same state-of-the-art polyamide FO membranes were used in the tests, which were run with real feed solutions and under varying conditions to observe the effect of initial flux, draw solution, and feed ionic composition. The results suggest that initial flux and calcium have the strongest influence on the extent of flux decline and recovery. The influence of different draw solutions in FO becomes apparent when the flux is relatively low. Analysis of the fouling indices and of the effective driving force, as well as direct observation of membranes following fouling, support the conclusion that the fouling behavior of the FO process is not necessarily better compared to an analogous hydraulic pressure-driven one, especially under relevant operational conditions and when the two processes work with similar fluxes.

Keywords: Forward osmosis; nanofiltration; fouling; organic foulants; calcium.

Highlights

- Permeation drag and feed ionic composition dominate organic fouling
- Calcium in the feed strongly enhances the detrimental effect of organic fouling
- Estimation of effective driving force, foulant resistance help analysis of behavior
- The nature of the driving force has a low impact on the fouling behavior
- Organic fouling is not necessarily less problematic in FO than in NF/RO

1. Introduction

Membrane-based separation technologies play an important role to address the challenge related to the increasing demand of freshwater [1]. Nanofiltration (NF) and reverse osmosis (RO) are established hydraulic pressure-driven (ΔP) membrane processes (PDMPs), already widely applied owing to their ability to produce high-quality water from wastewater effluents and sources with different salinity levels. In particular, NF has been proven valuable as a treatment system for the beneficial recovery of water from industrial effluents [2-4]. However, these technologies are prone to membrane fouling and careful pre-treatment is needed before for their effective deployment [5-7]. According to several investigations, innovative osmotically-driven membrane processes (ODMPs), for example, forward osmosis (FO), may help to overcome some of the obstacles related to fouling [8-10].

Numerous studies researched the performance of FO systems in the treatment of complex water sources, such as wastewaters with high organic content [11, 12]. The promising results observed in the application of FO may be mainly ascribed to (i) the use of highly selective and high-rejection membranes, with the concurrent (ii) alleged low fouling propensity resulting in resilient fluxes during filtration [13, 14]. The advantage of ODMPs over PDMPs in fouling behavior is the hypothesis that underlies much of the current research on FO, but numerous questions on this topic remain unanswered. Efforts have been made to provide accounts of the operating conditions influencing fouling in FO and evidences of the different performance related to fouling and cleaning observed when applying FO as opposed to PDMPs. Studies claim that the absence of a hydraulic pressure on the feed side results in a less compacted fouling layer on the FO membrane surface [15-17]. This phenomenon would result in a more stable flux during filtration and easier flux recovery upon cleaning. Investigations were also focused on addressing the possible existence of sustainable, critical, or threshold fluxes in FO [18-23]. For example, Nguyen *et al*. recently reported a study

related to the parameters influencing the achievement of a critical flux when using both asymmetric cellulose triacetate and polyamide-based thin-film composite (TFC) FO membranes [24]. At the same time, an increasing number of studies have been recently published, which suggest that ODMPs are not necessarily - or under all circumstances - superior to PDMPs when it comes to fouling behavior.

Recently, authors suggested that a more structured fouling layer may actually be associated with FO membranes compared to what observed in NF or RO, when working with same pressure gradient [25]. Another study suggested that the FO fouling propensity may be even worse than the RO behavior in the presence of specific foulants, such as alginate and silica [15]. Winson *et al.* stated that the advantageous fouling behavior of FO reported in the literature should be ascribed to the lower fluxes achievable in this process with respect to PDMPs, and not to the absence of an applied hydraulic pressure [26]. A robust study was also published by Siddiqui *et al.* [27], highlighting the importance of concentration polarization effects on fouling behavior and indicating that the FO vs. RO contest is in fact inherently more involved than a simple "win-or-lose engagement". Clearly, further efforts are required to address the complexity of these mechanisms and to provide more comprehensive answers to inform technology development and implementation.

Firstly, fouling is a multifaceted process involving numerous phenomena, for example, flux decline characterized by varying rate and extent, the possible existence and achievement of threshold fluxes, or the recovery of performance after cleaning steps. These phenomena should be analyzed separately and care should be taken when drawing conclusions that may only be valid for one or some of these fouling aspects. Moreover, consistent laboratory experiments should be performed when comparing ODMPs with PDMPs, by applying the same boundary conditions, for example, the same type of membranes and permeate flux. In addition, the nature of the draw solution plays an important role in foulant deposition and

accumulation, not relevant for PDMPs but doubtless essential when evaluating FO and ODMPs in general.

The aim of this research is thus to gain a better understanding of fouling in FO and to provide more support in the claims comparing the fouling behavior of this process with that in corresponding PDMP technologies. To achieve this goal, experiments are discussed that investigate the impact of three important fouling-influencing parameters: (i) initial permeate flux, (ii) feed solution composition, and (iii) draw solution composition. To enable a fair comparison between FO and NF, experiments are designed to deploy the same highly permeable TFC membranes and the same hydrodynamic conditions. Realistic operating conditions are explored and the results are analyzed through different fouling indicators related to flux decline and recovery, and through foulant inspection following filtration.

2. Materials and Methods

2.1 Feed composition and organic foulants

Two different feed solutions were employed to perform fouling experiments; see Table 1. Laboratory tap water was used as a real background solution. A synthetic background solution was also prepared by maintaining the same ionic composition and ionic strength determined for the tap water, but substituting calcium with sodium. The feed solutions were spiked with a nominal concentration of organic foulants equal to 300 mg/L, comprising an equal individual concentration (75 mg/L) of humic acids (HA), alginate (Alg), octanoic acid (OA), and bovine serum albumin (BSA), all purchased from Sigma-Aldrich (Milan, Italy). They were then filtered using a microfilter (0.45 μm) to eliminate all the undissolved substances and to represent previous contaminant removal steps preceding FO in a possible treatment train. Recently, proteins and humic substances were shown to have the greatest

contribution to irreversible fouling during the filtration of secondary wastewater by FO [28]. The characterization of the feed waters was performed by an external accredited company, Natura S.r.l. (Naples, Italy).

Table 1. Composition of the two water streams used as feed solutions, one with and the other without calcium ions, and concentrations of organic foulants.

Parameter	**Component**	**Tap water**	**Synthetic water without Ca^{2+}**
		Concentration	**Concentration**
Anions[c] (mg/L)	Cl^-	19.0	98.0
	NO_3^-	33.3	33.3
	SO_4^{2-}	52.0	52.0
	HCO_3^-	256.7	257.0
Cations[c] (mg/L)	Ca^{2+}	88.7	0.0
	Mg^{2+}	13.7	13.7
	Na^+	18.7	171.5
	K^+	1.3	1.3
	NH_4^+	0.1	0.1
Foulants (nominal concentration[a], mg/L)	Humic acids	75	
	Alginate	75	
	Octanoic acid	75	
	Bovine serum albumin	75	
Overall	**Measured pH**	**7.5 ± 0.2**	
	Resulting ionic strength (mM)	**9.74**	
	Resulting TDS (mg/L)	**640**	**694**
	Measured TOC[b] (mg/L)	**51.9 ± 4.6**	

[a]Based on the mass added into solution; [b]After microfiltration (see section 2.1). [c]The reported measurement error is <5%.

2.2 Lab units, membranes, and draw solutes

Fouling tests were performed with an FO and with an NF/RO laboratory system, already described in our previous publications [29, 30]. The FO setup was purchased from Sterlitech Corporation (Kent, WA, USA). It comprises two variable speed gear pumps (Cole-Parmer, Vernon Hills, IL), used to flow the feed and draw solutions in co-current mode. The temperature, conductivity, and cross-flow rate of both streams were recorded continuously

during filtration. The hydraulic pressure-driven (ΔP) system was run using a high-pressure pump (Hydra-cell pump, Wanner Engineering, Inc., Minneapolis, MN). Here, the retentate stream was recirculated back to the feed reservoir while the permeate stream was continuously collected in an external vessel. The cross-flow rate and the operating pressure were monitored and adjusted, independently of each other, by means of both a bypass valve and a back-pressure regulator. In all experiments, the permeate flux across the membrane was computed by recording the change in volume of the feed solution in time through a computer-interfaced balance, then dividing the resulting permeate flow rate by the active membrane area. The same custom-made flat-sheet membrane cell (previously described in [30]) was adopted in both FO and ΔP tests, with the aim to keep the same hydrodynamic conditions. A rectangular membrane sample of 22 cm^2 (3.4 sq. inches) can be housed in this cell. The hydrodynamic conditions in the feed channels during filtration corresponded to a Reynolds number of roughly 1500.

All the experiments were run with an initial feed volume of 6 L. The same volume of draw solution was used in FO experiments, obtained by dissolving the following single solutes in deionized (DI) water: sodium chloride, magnesium chloride, sodium sulfate, magnesium sulfate, or calcium chloride, all purchased from Carlo Erba (Milan, Italy). The initial volume of the feed solution (and of the draw solution) was chosen to have negligible loss (and gain) of water during the tests, thus keeping a near-constant nominal driving force. To further increase the robustness of the experiments, draw and feed concentrations were restored periodically in the first hours of each fouling experiment, by addition of concentrate stocks of solute and DI water in the draw and feed solution tanks, respectively, based on the measured volume of water permeated between each addition.

The same commercial TFC polyamide FO flat-sheet membranes were used in FO and ΔP filtration experiments. The average transport characteristics of the FO membrane were

obtained by following the protocol reported by Tiraferri *et al.* [31] and are reported in Table S1 of the Supporting Information (SI). Additional NF or RO fouling experiments were conducted with three membranes commercialized by DuPont (Wilmington, DE, USA): the NF90, XLE, and SW30HR membranes.

2.3 Operating conditions and protocols of the fouling experiments

Fouling experiments were performed under different operating conditions. One of the investigated conditions was the initial permeate flux: the same initial permeate fluxes in FO and in ΔP operation was obtained using appropriate draw solution concentrations in the former process and adjusting the feed hydraulic pressures in the latter case, as reported in Table 2. Please see Table S2 of the SI for the corresponding values of osmotic pressure in the FO experiments. For this first set of experiments, only NaCl was used as a draw solute in FO. A second set of experiments was performed in FO by changing the draw solute, with initial permeate flux equivalent to 15 or 30 L $m^{-2}h^{-1}$ (LMH).

Table 2. Summary of the operating conditions of the fouling tests. In FO, different draw solutes were used at the appropriate concentrations to achieve the desired initial flux values.

Process	**Parameter**	**Target initial permeate flux (L $m^{-2}h^{-1}$)**						
		7.5	**11.5**	**15**	**23**	**30**	**38**	**47**
FO (TFC polyamide membrane)	**Draw solute**	**Concentration (M)**						
	NaCl	0.12[a]	0.20[a]	0.31[b]	0.50[a]	1.15[b]	2.20[a]	3.50[a]
	$MgCl_2$			0.32[b]		1.05[b]		
	$CaCl_2$			0.27[b]		1.91[b]		
	Na_2SO_4			0.39[b]				
	$MgSO_4$			2.00[b]				
hydraulic pressure-driven (ΔP)	**Membrane**	**Hydraulic pressure (bar)**						
	TFC FO[c]	2.5[a]	3.5[a]	4[b]	6[a]	7.2[b]	10[a]	12[a]
	NF90					9.0[a]		
	XLE					9.5[a]		
	SW30HR					40[a]		

[a]Experiments conducted only with the feed solution containing calcium ion (real tap water); [b]Experiments conducted with both feed solutions; [c]Same as in FO experiments

Each experiment was run keeping a constant (i) cross-flow rate of 1.25 L/min (corresponding to a velocity of 0.25 m/s) and (ii) temperature of 25 °C. A test protocol was followed consisting of three phases, schematically depicted in Figure 1: (i) a stable flux phase, (ii) a fouling phase, and (iii) a flux recovery phase. The flux was firstly stabilized using the background solution as feed, without organic foulants (Jw_1). This stage allowed achievement of the hydrodynamic equilibrium and its duration depended on the type of membrane; FO membranes needed an overall stabilization of roughly 2.5 h, while NF90, XLE, and SW30HR were compacted for 6 h. The fouling phase then started at time zero, when the organic foulant stock solutions were added into the feed tank. This second phase was run for 20 h until a near stable flux was achieved, Jp. Subsequently, physical cleaning was performed by doubling the cross-flow rate of an organic-free feed solution to a value of 2.5 L/min and for a duration of 30 min before measuring again the water flux (Jw_2) under the same initial conditions, for about 3 h. Several experiments were carried out in duplicates and the results in terms of permeate flux were always replicable within a 5% confidence (± 5%).

The FO experimental results were combined with the prediction of a transport model (*vide infra*), to estimate the contribution of changes in bulk concentrations on flux decline. A control FO experiment was also performed with NaCl as draw solution and at the initial flux of 30 LMH without organic foulants in the feed solution. The results from this control test confirmed the adequacy of the model and, most importantly, showed a negligible flux decline when compared with fouling experiments (see Figure S1 in the Supporting Information). The modeling results and the control test demonstrated that the flux behavior observed during the fouling tests can be largely attributed to foulant deposition.

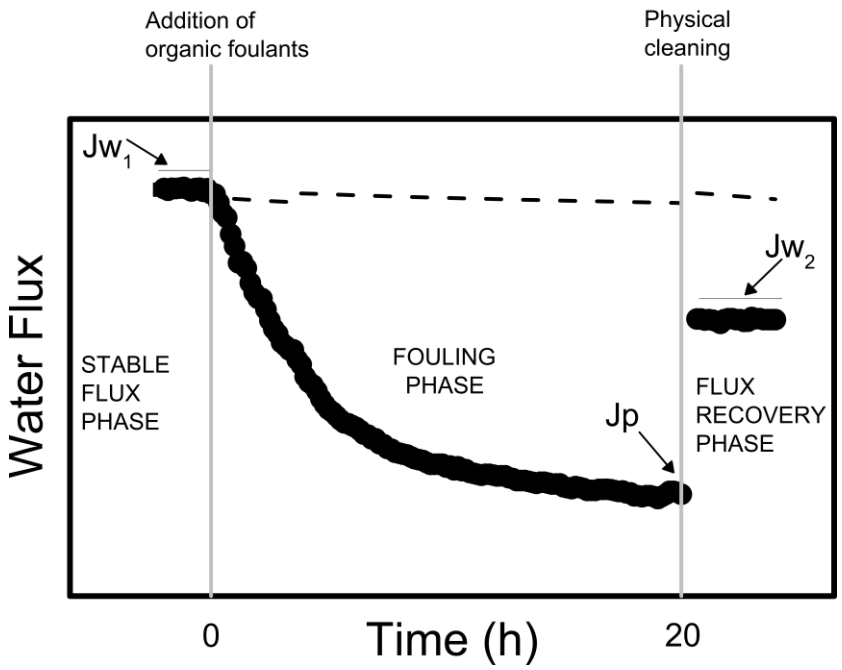

Figure 1. Representative experimental trace of the fouling tests, consisting of three stages: (i) the initial stabilization of flux, Jw_1, using the background feed solution; (ii) the fouling phase, which started at time zero with addition of organic foulants in the feed tank; (iii) the flux recovery phase, following physical cleaning, in which Jw_2 was measured with the same feed solution of the first stage. The dash line refers to the FO model applied to estimate the permeate flux accounting solely for the dilution of the draw solution and the concentration of the feed solution.

2.4 Image collection and analysis of the fouled membranes

Fouled membranes were stored in the respective feed, in absence of the organics, with further addition of 0.1 mM metabisulfite to keep the foulant characteristic while preventing any possible microorganism growth prior to analysis. For confocal microscopy, the fouling layer was stained with 50 µg/mL Concanavalin A with AlexaFluor 633 for 30 min and then gently rinsed with DI water. Fouling layers were visualized with a Leica SP8 laser scanning confocal microscope equipped with an HCX APO L U-V-I 20x/0.50 water immersion objective. Alexa Fluor 633 was excited with a 638 nm laser, and an emission window of 643

to 783 nm was used. Biomass was calculated from eight z-stacks using Comstat2 [32] with an automatic threshold determined using Otsu's method.

2.5 FO flux and system modeling

Simulations of the FO permeate flux were performed by applying the following equation 1 [30, 31]:

$$J_w^{FO} = A\left(\frac{\pi_D \exp\left(-\frac{J_w S}{D}\right) - \pi_F \exp\left(-\frac{J_w}{k}\right)}{1 + \frac{B}{J_w}\left[\exp\left(\frac{J_w}{k}\right) - \exp\left(-\frac{J_w S}{D}\right)\right]}\right) \quad (1)$$

Please note that this equation does not contain any adjustable parameter. Here, *A* is the active layer water permeance; *S*, *B*, and *D* represent the support layer structural parameter, the active layer salt permeability coefficient, and the diffusion coefficient of the draw solute in water, respectively. Table S1 of the SI summarizes the values of these parameters for the various draw solutes. The term *k* represents the mass transfer coefficient at the active layer–solution interface, which is a function of the hydrodynamics in the membrane flow cell and had value of 63.1 LMH in all the experiments and simulations [33]. To simplify this modeling, the real mixture of ionic species in the feed solution was replaced with the NaCl concentration that would produce the same osmotic pressure of the mixed solution.

Simulations were also performed to evaluate the changes of effective driving force and fouling resistance, R_f, during the filtration experiments. These two parameters were determined by applying equation 2 and 3, previously described by Siddiqui *et al*. [27], for hydraulic pressure-driven and for FO filtration experiments, respectively:

$$J_w^{NF} = \frac{\Delta p - \eta_{rej,f} \pi_F \exp\left(-\frac{J_w}{k_{ecp,f}}\right)}{\mu(R_m + R_f)} \quad (2)$$

$$J_w^{FO} = \frac{(\pi_D - \pi_F) - F_{ecp,f}(\pi_F + \frac{J_s}{J_w}\beta R_g T) - F_{dcp}(\pi_D + \frac{J_s}{J_w}\beta R_g T)}{\mu(R_m + R_f)} \quad (3)$$

In this model, the permeate flux is computed as function of the driving force (numerator) at the membrane surface (corrected by the concentration polarization effects) and the permeability to water derived by the viscosity of the feed solution and the overall mass transport resistance, exerted by both the membrane and the fouling layer (denominator). In equation 2, ΔP is the transmembrane pressure, η_{rej} is the solute rejection obtained from the conductivity values measured in the permeate and feed solutions, π_F is the osmotic pressure of the feed solution, J_w is the experimental permeate flux, and μ is the viscosity of the feed solution. The membrane resistance, R_m, is correlated to the water permeability coefficient through the simple equation: $R_m = 1/(\mu \cdot A)$. Equation 3 also incorporates the effect of reverse solute diffusion, J_s/J_w; Table S1 of the SI shows the values of this parameter for each of the draw solutes investigated in this study. In this equation, β represents the van't Hoff coefficient, R_g is the universal gas constant, and T is the absolute temperature. The terms $k_{ecp,f}$, $F_{ecp,f}$, and F_{dcp} represent the external and dilutive concentration polarization moduli in ΔP tests ($k_{ecp,f}$) and FO tests ($F_{ecp,f}$, F_{dcp}). In our study, the external concentration polarization at the feed side was not considered; this assumption was valid because of the low salt concentration of the feed solution, the relatively low permeate fluxes, and the high cross-flow velocity. Further justification for this assumption and additional considerations on this model are reported in Appendix A.

2.6 Fouling evaluation and fouling indices

Fouling indices were calculated to more easily evaluate the influence of different operating conditions on membrane fouling. In particular, at the end of each experiment, the

flux recovery ratio (FRR) and the total flux decline ratio (DRt) were determined with the following equations [34]:

$$\mathrm{FRR}(\%) = \frac{\mathrm{Jw_2}}{\mathrm{Jw_1}} \cdot 100 \qquad (4)$$

$$\mathrm{DRt} = \left(1 - \frac{\mathrm{Jp}}{\mathrm{Jw_1}}\right) \qquad (5)$$

The student t-Test was applied to assess whether the influence of certain parameters was statistically relevant. Statistical significance was assumed when the p-value with a two-tailed distribution for unequal variance between two separate sets of values was < 5%.

3. Results and discussion

3.1 Comparison of organic fouling effects in FO vs. hydraulic pressure-driven filtration

An experimental comparison of the organic fouling behavior in FO and ΔP processes is summarized in Figure 2. Specifically, Figure 2a, b reports the flux traces relative to the fouling stage of experiments performed in FO and ΔP tests starting from different initial fluxes. In both processes, a near stable flux was reached at the end of the fouling phase, J_p, possibly indicating the occurrence of a sustainable value, as suggested also by previous research [18-22]. While Field *et al.* defined a threshold flux as the limit between the low- and the high-fouling region, Bogler *et al.* suggested the existence of a steady-state value, which may be associated to the concepts of "sustainable" or "critical" flux [20, 33]. In this study, the values of J_p fell within a narrow range, between roughly 6 and 12 LMH, regardless of the driving force and without showing clear correlation with the initial flux. More specifically, FO fluxes converged to a similar or slightly lower value (7.6 ± 1.6 LMH) compared to those registered in ΔP experiments (9.1 ± 2.1 LMH). These results translated

into increasing values of the DRt index with increased initial flux for both processes; in addition, this index was similar or larger for FO compared to ΔP filtration tests (Figure 2d).

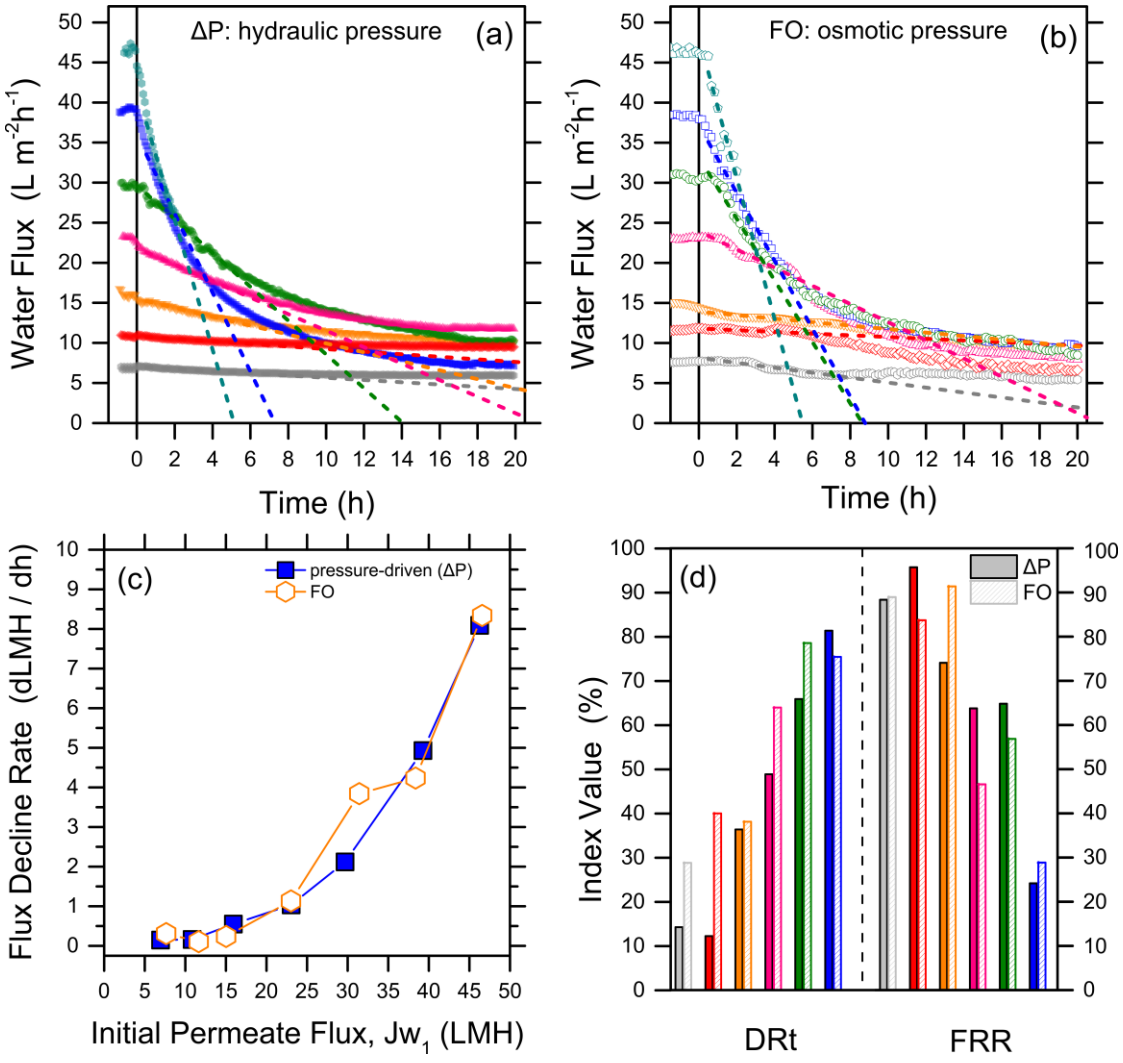

Figure 2. Comparison of fouling behavior between FO and a hydraulic pressure-driven (ΔP) process with a feed solution consisting of tap water spiked with organic foulants. The draw solute was NaCl in FO experiments. Experimental traces of flux decline in (a) ΔP filtration and (b) FO; here, the dash lines represent the best linear fit of the first 4 h of flux decline data. (c) Plot of the flux decline rates as a function of initial flux, Jw_1; the lines connecting the data points are plotted only as a guide for the eye. (d) Summary of the fouling indices: (left-hand half of the graph) DRt and (right-hand half) FRR, for (solid bars) ΔP and (pattern bars) FO processes.

Possibly a more consequential behavior for real application is that described by the fouling rate. The rates were estimated from the linear fit of the first 4 h of flux decline data and are plotted as a function of initial flux in Figure 2c (please note that the test associated with the highest initial flux of 46 LMH was run for 2 h, and the flux decline rate was estimated by fitting the data for this shorter time range compared to other tests). Below the initial flux of 15 LMH, the rate of flux decline due to fouling was negligible. Above this value, a superlinear (faster than linear) increase of flux decline rate as a function of initial flux was determined. Remarkably, the flux decline rates estimated for FO and ΔP filtrations overlapped almost perfectly.

Some considerations should be made regarding the occurrence of sustainable fluxes on the basis of the data presented in Figure 2. Under the conditions of this study, a threshold flux value (dividing rapid and slow flux decline regions) between 15 and 20 LMH may be identified. The critical flux (dividing behaviors of no flux decline and of flux decline) was instead low, possibly around 10 LMH. Running an FO system below the critical flux is suggested to be operationally beneficial, because fouling would be virtually absent or completely reversible under these conditions [20, 23, 24]. In contrast, it is worth noting that working with fluxes below 15 LMH would not be feasible because the cost of water would be too high with respect to capital and energy costs. This issue is especially true in applications that aim at the treatment of aqueous streams of low salinity and characterized by a significant amount of organic material (*e.g.*, wastewater), such as in this work, for which traditional technologies are still competitive. Previous studies identified critical FO fluxes in the range 20-25 LMH, which would leave sufficient opportunity for system optimization to find a balance between fouling minimization and maximization of productivity (*i.e.*, high fluxes). The same studies indicated that a strong inverse relation exists between organic foulant concentration in the feed water and the value of critical flux; also, they showed that mixtures

of organic foulants produce significantly worse effects than single foulants, such as more cohesive and compact fouling layers [23]. In this study, the feed water contained a relatively large concentration of foulants, which consisted of a complex mixture of four families of organic substances. These challenging conditions explain the fact that flux decline was always observed for economically feasible fluxes. Ultimately, the existence and the values of critical and threshold fluxes seem to be system-specific, but falling in a relatively narrow range between 10 and 25 LMH for FO concentrating feed streams that contain organic foulants and that fall in the category of wastewater effluents. As mentioned above, regardless of the occurrence of threshold or critical fluxes, the effects observed in this study were analogous in FO and in a process driven by hydraulic pressure.

The fouling tests provided comparable results in FO and in the ΔP process also in terms of flux recovery rate (FRR) (Figure 2d). Not unexpectedly, this parameter decreased with increasing initial flux, suggesting that the fouling layer was more difficult to remove by simple physical cleaning or that the resistance of the remaining layer was larger as the mass transport of foulants toward the membrane was favored at higher flux during the fouling phase. Overall, the results summarized in Figure 2 are in contrast with what reported by much of the current research on FO [15, 16]. Indeed, they indicate that driving the separation process by exploiting a transmembrane osmotic pressure does not necessarily translate into a better behavior compared to a hydraulic pressure-driven process when the operating conditions are equivalent, that is, the membrane and the productivity are the same. The permeation drag (*i.e.*, the force exerted on the foulants by the flow of solution that permeates through the membrane: this force is related to flux rather than driving force) seems more important to induce fouling and fouling-related detrimental effects compared to the nature of the driving force causing the drag itself [35]. This conclusion may in turn imply that the FO

process may not be advantageous with respect to NF or RO, at least in terms of organic fouling.

3.2 Influence of feed and draw solution composition on organic fouling in FO

An investigation of the influence of feed and draw solution composition on organic fouling was conducted to understand the operating conditions that may result in an improved FO fouling behavior. The analysis was carried out by performing filtration experiments with initial water fluxes of either 15 or 30 LMH. These values may be regarded as current boundaries of the FO technology: while 15 LMH represents a limit below which the process becomes economically unfeasible, fluxes larger than 30 LMH cannot be practically achieved with the currently available draw solutions and FO membranes, also considering the energy requirements of a downstream step to recover draw solutes at high concentration. Fouling tests were performed using different inorganic draw solutes and by changing the ionic composition of the feed solution. In Figure 3, the flux behavior of the respective ΔP tests is also reported for comparison with FO. A first interesting note concerns the ability of the FO model to predict the experimental initial flux data with great accuracy. As reported by previous research [29, 30], FO simulations based simply on equation 1 are a useful tool to predict the productivity of an FO system with the assumption of clean membranes.

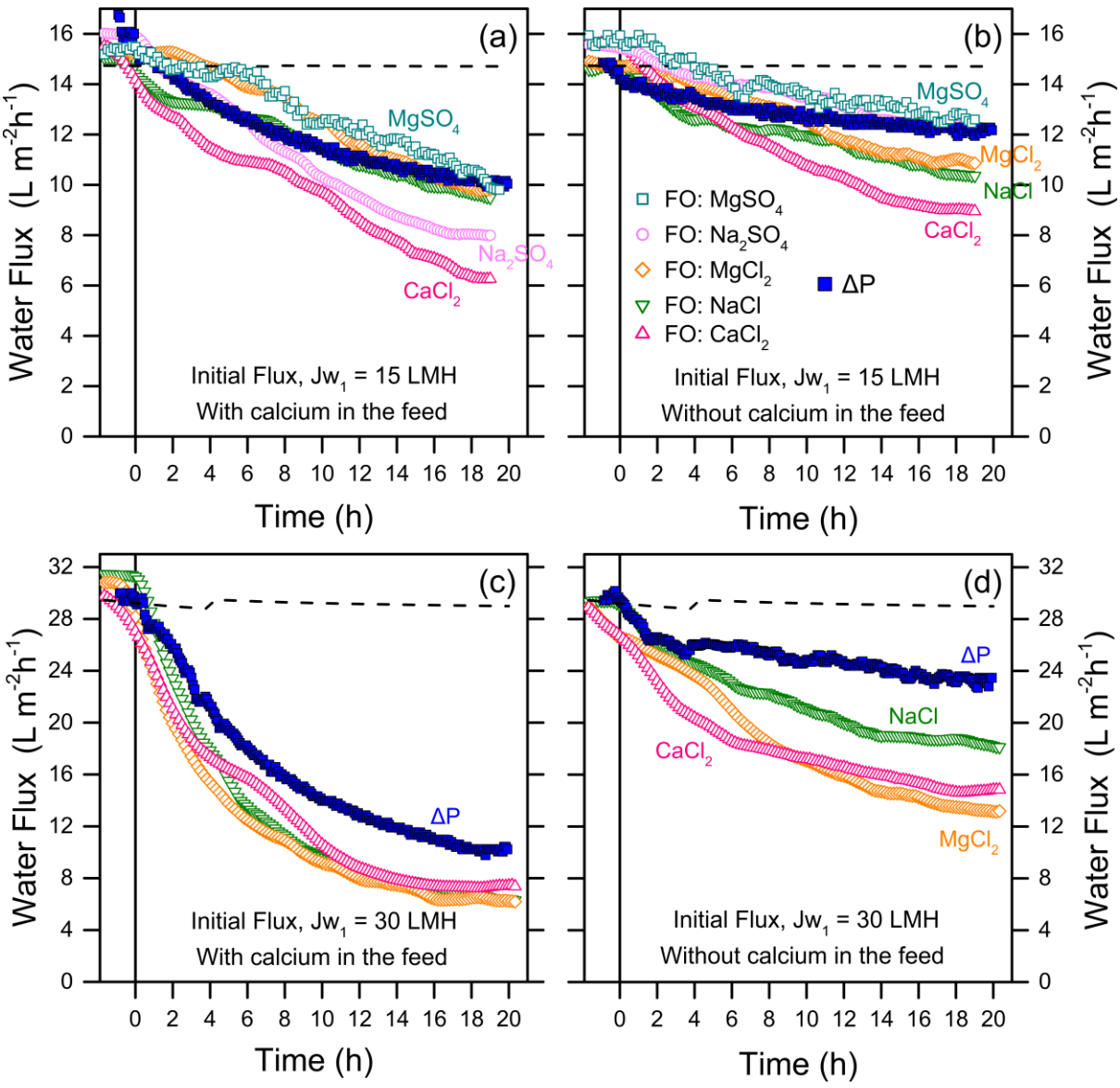

Figure 3. Results of fouling experiments performed in hydraulic pressure-driven (ΔP) filtration and in FO with different draw solutions (Table 1). Top row: experiments conducted at initial permeate flux, Jw_1, of 15 L $m^{-2}h^{-1}$ with (a) real feed water in the presence of calcium and (b) in the mimicked water without calcium. Bottom row: experiments conducted at larger initial permeate flux, Jw_1, of 30 L $m^{-2}h^{-1}$ (c) with real feed water in the presence of calcium and (d) in the mimicked water without calcium. The dash lines refer to the model prediction of permeate flux based solely on the dilution of the NaCl draw solution and the concentration of the feed solution. The legend shown in (b) is valid for all the graphs.

Overall, the data indicate that organic fouling in both FO and ΔP tests was strongly influenced by the presence of calcium, consistent with previous observations [36-38]. These results are commonly rationalized with the capacity of calcium ions to complex with carboxyl-rich organic materials and to cross-link these substances with the carboxyl groups of polyamide membranes [39, 40]. In this study, the detrimental effect of calcium was enhanced at high initial flux, as suggested by a comparison of the data presented in Figure 3c and 3d. Remarkably, under conditions of high flux and in the presence of calcium in the feed solution, the nature of the inorganic draw solute did not seem to play any role on flux decline (Figure 3c). The influence of the draw solution was only visible when the initial flux was low. In particular, chloride-based draw solutes induced a larger flux decline compared to sulfate-based solutes when filtering a feed solution without calcium (Figure 3b and Figure S2b of the SI). This observation may be reasonably explained with a greater tendency of chloride ions to reversely diffuse into the feed solution, thus enhancing the local ionic strength at the membrane-feed interface and promoting foulant deposition and the formation of a denser cake layer [41]. In contrast, when calcium was present in the feed solution (Figure 3a and Figure S2a of the SI), a larger rate of flux decline was observed for the sulfate-based draw solutions, rationalized with the co-deposition of gypsum at the membrane-feed interface [39]. Indeed, this phenomenon was more important when Na_2SO_4 instead of $MgSO_4$ was employed, due to the higher reverse diffusion of the former salt comprising the monovalent counterion. Clearly, when calcium chloride was used as draw solute, the flux decline was the fastest due to the contribution of calcium from reverse salt flux. Please note that recent reports have suggested that organic fouling layers may cause a reduction in reserve salt flux [42]. This phenomenon may diminish the influence of draw solutes on further organic fouling behavior and may partly be the reason for the observations of this

study: reverse salt flux may be sufficiently large to influence organic fouling behavior only when the fouling layer is not pronounced, that is, at low initial flux.

Comparing the curves obtained in tests employing different driving forces, a lower flux decline was generally observed in the ΔP processes, especially when the experiments were operated at the higher initial flux, namely, 30 LMH. The flux recovery ratios had similar values in FO and ΔP tests (Figure S2 of the SI). These somewhat surprising results are nonetheless in accordance with what discussed in section 3.1. Usually, when the fouling in FO is compared to that in NF or RO, different membranes are applied. To assess the influence of the membrane and that of applied pressure on flux decline, additional hydraulic pressure-driven experiments were carried out with three commercial polyamide-based membranes of different density. The results from these tests are reported in Figure S3 of the SI. No or negligible effect of applied pressure was observed and the three commercial membranes had similar behavior in terms of both flux decline and recovery, regardless of the magnitude of the driving force. Actually, the fouling tendency of the FO membrane was higher compared to that of the three NF/RO membranes, even if the former was operated at lower applied pressure, suggesting that organic fouling under the conditions of this study was possibly more related to the nature of the membrane rather than that of the driving force. This conclusion implies that comparisons of the fouling behavior in PDMPs and ODMPs operated with different membranes may not be applicable or may not be valid under all circumstances.

3.3 Analysis of the effective driving force and foulant resistance

The results collected so far suggest that there is no particular disadvantage of PDMPs in terms of organic fouling when compared with FO, specifically in the range of interest for FO applications. To understand the reasons of such observations, an analysis was performed by applying equations 2 and 3 to the experimental data. Figure 4a and 4b present the calculated

effective driving force and fouling resistance (R_f), respectively, as a function of time during tests performed at initial flux of 15 and 30 LMH. The effective driving force represents here the pressure (hydraulic or osmotic) difference across the combined polyamide active layer and foulant layer. The available force for permeation is decreased significantly by the resistance exerted by the fouling layer, thus resulting in a lower trans-polyamide layer pressure differential, which is the force ultimately accountable for water flux.

The calculated value of effective driving force in our study is constant for ΔP filtration experiments and nearly coincides with the nominal driving force, namely, the applied hydraulic pressure. On the other hand, this parameter is considerably lower than the nominal driving force (*i.e.*, the bulk osmotic pressure of the draw solution) in the beginning of the FO experiments, when the water flux is still high. The effective driving force increases as the water flux is reduced following fouling, due to the ICP self-compensation effect [18, 27, 43], and it tends to reach the value of bulk osmotic pressure (Table S2 of the SI) as the water flux gets closer to zero.

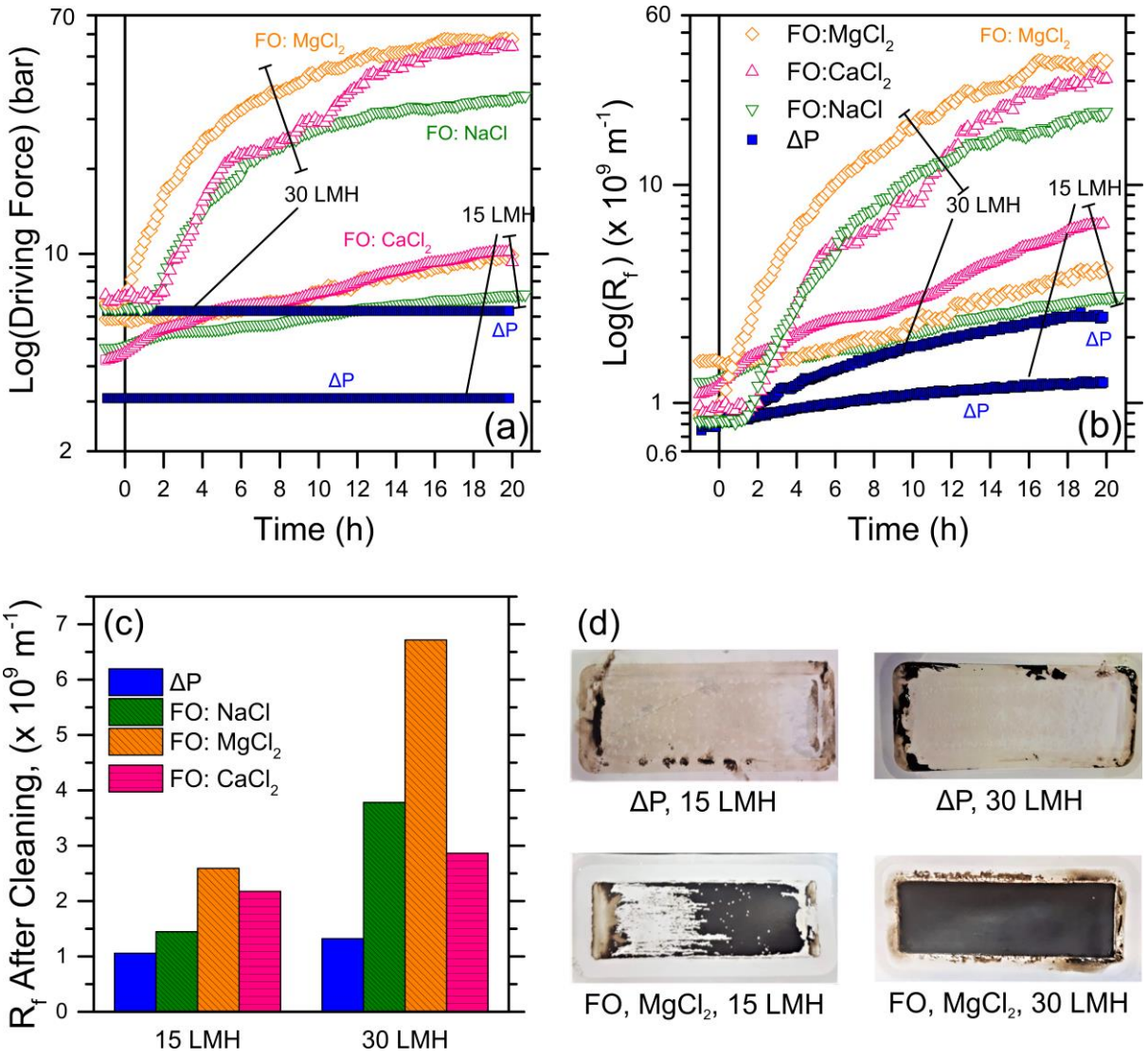

Figure 4. Calculated (a) effective driving force and (b) fouling resistance (R_f) from the data reported in Figure 3, with calcium present in the feed solution. In (c), the calculated fouling resistance after physical cleaning is shown. (d) Color photographs of membrane samples following fouling and cleaning from FO and hydraulic pressure-driven (ΔP) filtration tests at both values of initial flux, related to the orange and blue bars in graph (c).

The increase of effective driving force in FO was largely independent of the nature of the draw solute (Figure 4a) and, most importantly, led to an increase of the permeation drag with the consequent development of the fouling resistance, R_f (Figure 4b). Another important aspect to take into account is the negligible effect of external concentration polarization

(ECP) on the effective driving force, in agreement with previous studies [10, 18, 27]; see SI section S4. The calculations shown in Figure 4 imply a similar water flux decline in FO and ΔP processes, but with a substantial difference in terms of fouling layer resistance on the membrane surface, which seems to be much more pronounced in FO; see also Figure 4c for the value of fouling layer resistance determined after physical cleaning. The modeling results were corroborated by simple observation of the membranes, some reported in Figure 4d: membrane samples used in FO tests were nearly always coated by a uniform foulant layer, even following cleaning, while this layer was less evident or present following ΔP filtration [21, 44-46]. Overall, the results suggest that the permeation drag has a dominant contribution to fouling and fouling-related detrimental effects, possibly due to the increase of calcium and foulant transport and accumulation onto the membrane surface. This phenomenon is independent of the nature of the driving force.

3.4 Overall summary of the fouling behavior and comparison between FO and hydraulic pressure-driven tests

It may be worth presenting a review of the results discussed so far with a concise statistical analysis of the main factors affecting organic fouling in FO. The data plotted in Figure 5a and 5b are average values determined by lumping together the indices previously presented and classified based on the presence of calcium in the feed and on the initial flux. There was statistically significant difference ($p = 0.02$) in the flux decline ratios obtained in tests performed at low vs. high initial flux when the feed contained calcium; no significant difference ($p = 0.08$) when calcium was absent (Figure 5a, DRt). Similarly, only at high flux the DRt index was statistically ($p = 0.02$) higher for feeds comprising calcium compared to feeds in the absence of this multivalent cation (Figure 5b, DRt). These agreeing observations may be rationalized with the important effect of convection of calcium and organic foulants onto the membranes. On the other hand, the difference in flux recovery ratios was

statistically significant (p = 0.03) between tests run at low vs. high flux only in the absence of calcium (Figure 5a, FRR). The influence of calcium on FRR was instead significant (p = 0.04) at low flux (Figure 5b, FRR). This result is in agreement with what observed with the confocal microscope (Figure S5 in the Supporting Information), which showed a lower thickness of the foulant layer on the membrane used to filter a feed solution with calcium. Due to the cross-linking capability of calcium, its presence can induce the formation of a more compact and thinner cake layer on the membrane surface [47, 48], which was observed even after physical cleaning.

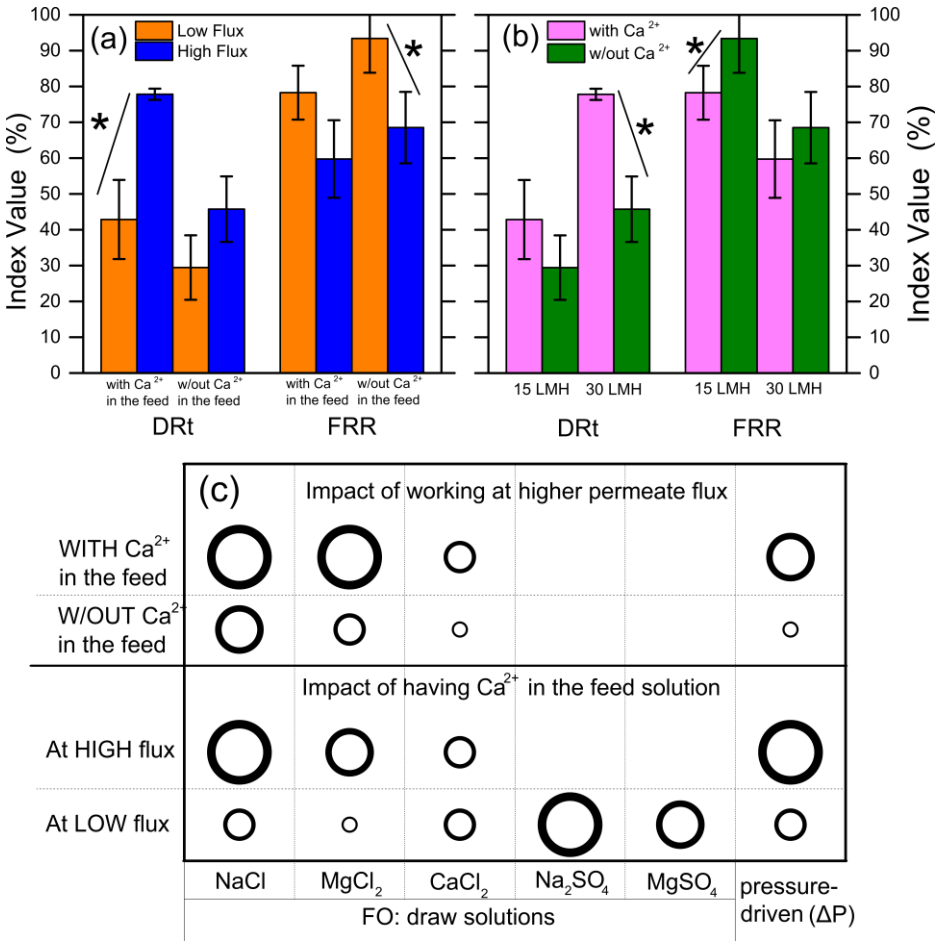

Figure 5. Average values of the fouling indices obtained in FO experiments. Graph (a) allows assessing the differences between experiments performed at (orange) low initial flux and (blue) high initial flux. Graph (b) allows assessing the differences between experiments (light pink) without and (green) with calcium in the feed solution. The asterisk indicates a statistically significant difference

($p < 0.05$ based on t-Test) between data represented by adjacent bars. (c) Qualitative assessment of the influence of flux and feed calcium ions under different filtration conditions; here, the circle diameter is proportional to the overall negative impact on the process performance. N.B.: the circle diameter does not refer to the process performance or fouling behavior in absolute terms.

Figure 5c attempts to recapitulate the mechanisms discussed above with the goal to inform the choice of the operating conditions in FO and minimize organic fouling. Regardless of the nature of the draw solute, the figure summarizes similar fouling trends in FO and ΔP filtrations, highlighting the key role of the feed solution composition and the permeation drag on fouling behavior. In the presence of calcium in the feed solution, more extensive pre-treatment should be evaluated and recurring chemical cleanings may be needed to enhance the productivity of a system working at high average water fluxes. Regarding the possible draw solutions to be employed in FO, the use of antiscalants with sulfate- based DS may be critical, while magnesium chloride would be slightly preferred over sodium chloride to work at medium-high water fluxes.

4. Concluding remarks

This study presented an analysis of organic fouling in forward osmosis and an even-handed comparison with a hydraulic pressure-driven (ΔP) membrane processes, namely, nanofiltration, under analogous conditions and productivity. In summary, the permeation drag, rather than the nature of the driving force, was found to play a dominant role in the fouling behavior of both FO and ΔP filtrations. The presence of calcium in the feed solution also importantly increased organic fouling. In FO, the feed ionic composition outweighed the effect of draw solution composition at economically feasible values of water flux. Indeed, at higher fluxes the permeation drag is higher, thus enhancing calcium and foulants transport toward the membrane surface. Draw solutes comprising sulfate anions can only guarantee

low to medium water fluxes in FO, due to their low solubility and osmotic potential; they should be avoided when calcium is present in the feed solution due to the possible formation of gypsum at the membrane/feed interface. Among the inorganic draw solutes investigated, magnesium chloride seemed to be the most promising one, as it was able to produce high fluxes while minimizing organic fouling.

Interestingly, the nature of the driving force did not contribute to a difference in organic fouling behavior. It follows that FO and ΔP processes would be characterized by similar organic fouling-related effects, at least under conditions comparable to this study. This conclusion is not in accordance with what presented or indicated by numerous previous studies, which have pointed to layer compaction as the main culprit for the more "malicious" behavior of fouling in ΔP membrane processes. No direct effect of foulant compaction was observed here; as a matter of fact, confocal microscopy data indicated instead overall thicker foulant layers at the end of ΔP tests, where remaining on the samples (Figure S5 of the SI). Even assuming that the effect of compaction is important under different conditions or for other applications, an often overlooked issue seems to be the following: with analogous membranes, relatively low values of hydraulic pressure are needed in ΔP tests to achieve the same fluxes and rejection rates observed in FO (the loss of effective driving force is much larger in FO, due to the impact of dilutive ICP), thus constraining the alleged detrimental effect of fouling layer compaction.

Please also note that, with the goal to produce high-quality water, a downstream draw solute/water separation stage is needed following the FO step, which extracts water by diluting a draw solution. In this sense, FO may be thought of as a high-end pre-treatment option for a subsequent purification process, with the advantage of providing a highly selective barrier to contaminants since FO membranes are nearly as selective as reverse osmosis membranes currently used for desalination of medium to high salinity feed waters.

From a thermodynamics point of view, an FO-based treatment train always requires more energy than a simple RO step challenged by the same feed water. Nevertheless, deploying FO may truly be beneficial if the fouling behavior of this process is obviously advantageous compared to that of an equivalent RO system and/or if the target product water needs to respect very stringent limits, thus justifying the choice of a multi-barrier approach. The use of FO may also be advantageous if a window of sustainable flux (below critical or threshold values) can be identified that allow effective control of fouling-related problems while simultaneously being of sufficiently high magnitude to justify system costs. However, from an operational standpoint, if or when no fouling advantage exists, as observed in this study, we surmise that an FO based system will never be favorable compared to an RO process, or even a combined ultrafiltration-RO treatment train, owing to higher energy costs of the FO-based system and the need for the same cleaning schemes. Decisions to deploy an FO-based system train instead of an RO-based train should thus not be based on the pre-assumption of a superior fouling behavior, but on real evidence of better fouling behavior of the former, combined with other boundary conditions, such as the required water product quality, the need for and extent of a draw solution regeneration steps, and other site-specific considerations.

Acknowledgments

M.G. thanks Politecnico di Torino for financial support for expenses while visiting Montana Technological University. The authors thank Carson Bechtel for confocal microscopy data curation and Comstat analyses. This material is partly based upon work supported by the National Science Foundation under Grant No. 1828523. Any opinions, findings, and

conclusions or recommendations expressed in this material are those of the author(s) and do not necessarily reflect the views of the National Science Foundation.

References

[1] R. Rautenbach, R. Albrecht, Membrane Processes, Wiley, 1989.

[2] Z.B. Gönder, S. Arayici, H. Barlas, Advanced treatment of pulp and paper mill wastewater by nanofiltration process: Effects of operating conditions on membrane fouling, Sep. Purif. Technol., 76 (2011) 292-302. https://doi.org/10.1016/j.seppur.2010.10.018

[3] C. Tang, V. Chen, Nanofiltration of textile wastewater for water reuse, Desalination, 143 (2002) 11-20. https://doi.org/10.1016/S0011-9164(02)00216-3

[4] J. Gozálvez-Zafrilla, D. Sanz-Escribano, J. Lora-García, M.L. Hidalgo, Nanofiltration of secondary effluent for wastewater reuse in the textile industry, Desalination, 222 (2008) 272-279. https://doi.org/10.1016/j.desal.2007.01.173

[5] B. Van der Bruggen, C. Vandecasteele, T. Van Gestel, W. Doyen, R. Leysen, A review of pressure-driven membrane processes in wastewater treatment and drinking water production, Environ. Prog., 22 (2003) 46-56. https://doi.org/10.1002/ep.670220116

[6] J.H. Jhaveri, Z. Murthy, A comprehensive review on anti-fouling nanocomposite membranes for pressure driven membrane separation processes, Desalination, 379 (2016) 137-154. https://doi.org/10.1016/j.desal.2015.11.009

[7] S. Shirazi, C.-J. Lin, D. Chen, Inorganic fouling of pressure-driven membrane processes—a critical review, Desalination, 250 (2010) 236-248. https://doi.org/10.1016/j.desal.2009.02.056

[8] T.Y. Cath, A.E. Childress, M. Elimelech, Forward osmosis: principles, applications, and recent developments, J. Membr. Sci., 281 (2006) 70-87. https://doi.org/10.1016/j.memsci.2006.05.048

[9] J.-J. Qin, B. Liberman, K. A Kekre, A. Gossan, Direct osmosis for reverse osmosis fouling control: principles, applications and recent developments, Open Chem. Eng. J., 3 (2009). https://doi.org/10.2174/1874123100903010008

[10] Q.H. She, R. Wang, A.G. Fane, C.Y.Y. Tang, Membrane fouling in osmotically driven membrane processes: A review, J. Membr. Sci., 499 (2016) 201-233. https://doi.org/10.1016/j.memsci.2015.10.040

[11] D.L. Shaffer, L.H. Arias Chavez, M. Ben-Sasson, S. Romero-Vargas Castrillón, N.Y. Yip, M. Elimelech, Desalination and reuse of high-salinity shale gas produced water: drivers, technologies, and future directions, Environ. Sci. Technol., 47 (2013) 9569-9583. https://doi.org/10.1021/es401966e

[12] F. Zhang, K.S. Brastad, Z. He, Integrating Forward Osmosis into Microbial Fuel Cells for Wastewater Treatment, Water Extraction and Bioelectricity Generation, Environ. Sci. Technol., 45 (2011) 6690-6696. https://doi.org/10.1021/es201505t

[13] E. Akhondi, F. Wicaksana, A.G. Fane, Evaluation of fouling deposition, fouling reversibility and energy consumption of submerged hollow fiber membrane systems with

periodic backwash, J. Membr. Sci., 452 (2014) 319-331. https://doi.org/10.1016/j.memsci.2013.10.031

[14] S. Yadav, I. Ibrar, S. Balky, D. Khanafer, A. Altaee, C. Padmanaban, A. Kumar Samal, A.H. Hawari, Organic Fouling in Forward Osmosis: A Comprehensive Review, Water, 12 (2020) 1505. https://doi.org/10.3390/w12051505

[15] Y. Jang, H. Cho, Y. Shin, Y. Choi, S. Lee, J. Koo, Comparison of fouling propensity and physical cleaning effect in forward osmosis, reverse osmosis, and membrane distillation, Desalin. Water Treat., 57 (2016) 24532-24541. https://doi.org/10.1080/19443994.2016.1152650

[16] Y. Kim, M. Elimelech, H.K. Shon, S. Hong, Combined organic and colloidal fouling in forward osmosis: Fouling reversibility and the role of applied pressure, J. Membr. Sci., 460 (2014) 206-212. https://doi.org/10.1016/j.memsci.2014.02.038

[17] M.D. Firouzjaei, S.F. Seyedpour, S.A. Aktij, M. Giagnorio, N. Bazrafshan, A. Mollahosseini, F. Samadi, S. Ahmadalipour, F.D. Firouzjaei, M.R. Esfahani, A. Tiraferri, M. Elliott, M. Sangermano, A. Abdelrasoul, J.R. McCutcheon, M. Sadrzadeh, A.R. Esfahani, A. Rahimpour, Recent Advances in Functionalized Polymer Membranes for Biofouling Control and Mitigation in Forward Osmosis, J. Membr. Sci., 596 (2020) 117604. https://doi.org/10.1016/j.memsci.2019.117604

[18] W.C. Lay, T.H. Chong, C.Y. Tang, A.G. Fane, J. Zhang, Y. Liu, Fouling propensity of forward osmosis: investigation of the slower flux decline phenomenon, Water Sci. Technol., 61 (2010) 927-936. https://doi.org/10.2166/wst.2010.835

[19] N.W. Diagne, M. Rabiller-Baudry, L. Paugam, On the actual cleanability of polyethersulfone membrane fouled by proteins at critical or limiting flux, J. Membr. Sci., 425 (2013) 40-47. https://doi.org/10.1016/j.memsci.2012.09.001

[20] R.W. Field, G.K. Pearce, Critical, sustainable and threshold fluxes for membrane filtration with water industry applications, Adv. Colloid Interface Sci., 164 (2011) 38-44. https://doi.org/10.1016/j.cis.2010.12.008

[21] Y.N. Wang, F. Wicaksana, C.Y. Tang, A.G. Fane, Direct Microscopic Observation of Forward Osmosis Membrane Fouling, Environ. Sci. Technol., 44 (2010) 7102-7109. https://doi.org/10.1021/es101966m

[22] S.F. Zhao, L.D. Zou, D. Mulcahy, Effects of membrane orientation on process performance in forward osmosis applications, J. Membr. Sci., 382 (2011) 308-315. https://doi.org/10.1016/j.memsci.2011.08.020

[23] T.-T. Nguyen, C. Lee, R.W. Field, I.S. Kim, Insight into organic fouling behavior in polyamide thin-film composite forward osmosis membrane: Critical flux and its impact on the economics of water reclamation, J. Membr. Sci., 606 (2020) 118118. https://doi.org/10.1016/j.memsci.2020.118118

[24] T.-T. Nguyen, S. Kook, C. Lee, R.W. Field, I.S. Kim, Critical flux-based membrane fouling control of forward osmosis: Behavior, sustainability, and reversibility, J. Membr. Sci., 570 (2019) 380-393. https://doi.org/10.1016/j.memsci.2018.10.062

[25] M.S. Toran, A. D'Haese, I. Rodríguez-Roda, W. Gernjak, Fouling propensity of novel TFC membranes with different osmotic and hydraulic pressure driving forces, Water Res. , (2020) 115657. https://doi.org/10.1016/j.watres.2020.115657

[26] H. Alegre, Is strategic asset management applicable to small and medium utilities?, Water Sci. Technol., 62 (2010) 2051-2058. https://doi.org/10.2166/wst.2010.509

[27] F.A. Siddiqui, Q.H. She, A.G. Fane, R.W. Field, Exploring the differences between forward osmosis and reverse osmosis fouling, J. Membr. Sci., 565 (2018) 241-253. https://doi.org/10.1016/j.memsci.2018.08.034

[28] M. Zhan, G. Gwak, D.I. Kim, K. Park, S. Hong, Quantitative analysis of the irreversible membrane fouling of forward osmosis during wastewater reclamation: Correlation with the modified fouling index, J. Membr. Sci., 597 (2020) 117757. https://doi.org/10.1016/j.memsci.2019.117757

[29] M. Giagnorio, F. Ricceri, A. Tiraferri, Desalination of brackish groundwater and reuse of wastewater by forward osmosis coupled with nanofiltration for draw solution recovery, Water Res., 153 (2019) 134-143. https://doi.org/10.1016/j.watres.2019.01.014

[30] M. Giagnorio, F. Ricceri, M. Tagliabue, L. Zaninetta, A. Tiraferri, Hybrid Forward Osmosis-Nanofiltration for Wastewater Reuse: System Design, Membranes, 9 (2019). https://doi.org/10.3390/Membranes9050061

[31] A. Tiraferri, N.Y. Yip, A.P. Straub, S. Romero-Vargas Castrillon, M. Elimelech, A Method for the Simultaneous Determination of Transport and Structural Parameters of Forward Osmosis Membranes, J. Membr. Sci., 444 (2013) 523-538. https://doi.org/10.1016/j.memsci.2013.05.023

[32] A. Heydorn, A.T. Nielsen, M. Hentzer, C. Sternberg, M. Givskov, B.K. Ersbøll, S. Molin, Quantification of biofilm structures by the novel computer program COMSTAT, Microbiology, 146 (2000) 2395-2407. https://doi.org/10.1099/00221287-146-10-2395

[33] E. Bar-Zeev, K.R. Zodrow, S.E. Kwan, M. Elimelech, The importance of microscopic characterization of membrane biofilms in an unconfined environment, Desalination, 348 (2014) 8-15. https://doi.org/10.1016/j.desal.2014.06.003

[34] Q. Wu, A. Tiraferri, H. Wu, W. Xie, B. Liu, Improving the Performance of PVDF/PVDF-g-PEGMA Ultrafiltration Membranes by Partial Solvent Substitution with Green Solvent Dimethyl Sulfoxide during Fabrication, ACS Omega, 4 (2019) 19799-19807. https://doi.org/10.1021/acsomega.9b02674

[35] G.Z. Ramon, E.M.V. Hoek, On the enhanced drag force induced by permeation through a filtration membrane, J. Membr. Sci., 392-393 (2012) 1-8. https://doi.org/10.1016/j.memsci.2011.10.056

[36] P. van den Brink, A. Zwijnenburg, G. Smith, H. Temmink, M. van Loosdrecht, Effect of free calcium concentration and ionic strength on alginate fouling in cross-flow membrane filtration, J. Membr. Sci., 345 (2009) 207-216. https://doi.org/10.1016/j.memsci.2009.08.046

[37] H. Mo, K.G. Tay, H.Y. Ng, Fouling of reverse osmosis membrane by protein (BSA): Effects of pH, calcium, magnesium, ionic strength and temperature, J. Membr. Sci., 315 (2008) 28-35. https://doi.org/10.1016/j.memsci.2008.02.002

[38] Y.H. Mo, K. Xiao, Y.X. Shen, X. Huang, A new perspective on the effect of complexation between calcium and alginate on fouling during nanofiltration, Sep. Purif. Technol., 82 (2011) 121-127. https://doi.org/10.1016/j.seppur.2011.08.033

[39] M. Xie, S.R. Gray, Gypsum scaling in forward osmosis: Role of membrane surface chemistry, J. Membr. Sci., 513 (2016) 250-259. https://doi.org/10.1016/j.memsci.2016.04.022

[40] M.M. Zhang, Q.H. She, X.L. Yan, C.Y. Tang, Effect of reverse solute diffusion on scaling in forward osmosis: A new control strategy by tailoring draw solution chemistry, Desalination, 401 (2017) 230-237. https://doi.org/10.1016/j.desal.2016.08.014

[41] Q. Ge, M. Ling, T.-S. Chung, Draw solutions for forward osmosis processes: developments, challenges, and prospects for the future, J. Membr. Sci., 442 (2013) 225-237. https://doi.org/10.1016/j.memsci.2013.03.046

[42] L.H. Kim, S.S. Bucs, G.-J. Witkamp, J.S. Vrouwenvelder, Organic composition in feed solution of forward osmosis membrane systems has no impact on the boron and water flux but reduces scaling, J. Membr. Sci., 611 (2020) 118306. https://doi.org/10.1016/j.memsci.2020.118306

[43] C.Y.Y. Tang, Q.H. She, W.C.L. Lay, R. Wang, A.G. Fane, Coupled effects of internal concentration polarization and fouling on flux behavior of forward osmosis membranes during humic acid filtration, J. Membr. Sci., 354 (2010) 123-133. https://doi.org/10.1016/j.memsci.2010.02.059

[44] Y. Gu, Y.-N. Wang, J. Wei, C.Y. Tang, Organic fouling of thin-film composite polyamide and cellulose triacetate forward osmosis membranes by oppositely charged macromolecules, Water Res., 47 (2013) 1867-1874. https://doi.org/10.1016/j.watres.2013.01.008

[45] B. Mi, M. Elimelech, Chemical and physical aspects of organic fouling of forward osmosis membranes, J. Membr. Sci., 320 (2008) 292-302. https://doi.org/10.1016/j.memsci.2008.04.036

[46] C.Y. Tang, Y.-N. Kwon, J.O. Leckie, The role of foulant–foulant electrostatic interaction on limiting flux for RO and NF membranes during humic acid fouling—theoretical basis, experimental evidence, and AFM interaction force measurement, J. Membr. Sci., 326 (2009) 526-532. https://doi.org/10.1016/j.memsci.2008.10.043

[47] I. Szilagyi, G. Trefalt, A. Tiraferri, P. Maroni, M. Borkovec, Polyelectrolyte adsorption, interparticle forces, and colloidal aggregation, Soft Matter, 10 (2014) 2479-2502. https://doi.org/10.1039/c3sm52132j

[48] A.I. Schafer, A.G. Fane, T.D. Waite, Nanofiltration of natural organic matter: Removal, fouling and the influence of multivalent ions, Desalination, 118 (1998) 109-122. https://doi.org/10.1016/S0011-9164(98)00104-0
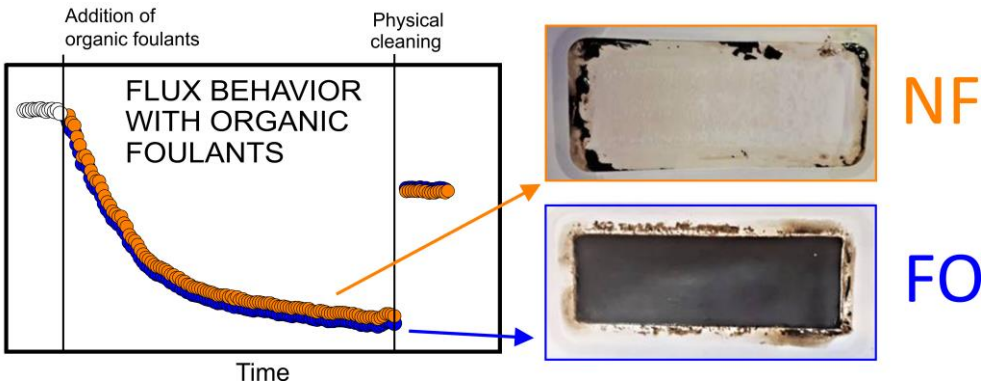
Graphical Abstract